Vol. 13, pp. 77–84 (2016)
doi: 10.2142/biophysico.13.0_77

Biophysics and Physicobiology
https://www.jstage.jst.go.jp/browse/biophysico/

Regular Article

Molecular mechanisms of substrate specificities of uridine-cytidine kinase

Wataru Tanaka[1], Mitsuo Shoji[1,2], Fumiaki Tomoike[3], Yuzuru Ujiie[1], Kyohei Hanaoka[1], Ryuhei Harada[1], Megumi Kayanuma[1,2], Katsumasa Kamiya[4], Toyokazu Ishida[5], Ryoji Masui[6,7], Seiki Kuramitsu[6] and Yasuteru Shigeta[1,2]

[1]*Graduate School of Pure and Applied Sciences, University of Tsukuba, Tsukuba, Ibaraki 305-8571, Japan*
[2]*Center for Computational Sciences, University of Tsukuba, Tsukuba, Ibaraki 305-8577, Japan*
[3]*Graduate School of Frontier Biosciences, Osaka University, Suita, Osaka 565-0871, Japan*
[4]*Center for Basic Education and Integrated Learning, Kanagawa Institute of Technology, Atsugi, Kanagawa 243-0292, Japan*
[5]*Nanosystem Research Institute, National Institute of Advanced Industrial Science and Technology (AIST), Tsukuba, Ibaraki 305-8568, Japan*
[6]*Graduate School of Science, Osaka University, Toyonaka, Osaka 560-0043, Japan*
[7]*Graduate School of Science, Osaka City University, Sumiyoshi-ku, Osaka 558-8585, Japan*

Received March 31, 2016; accepted May 10, 2016

A uridine-cytidine kinase (UCK) catalyzes the phosphorylation of uridine (Urd) and cytidine (Cyd) and plays a significant role in the pyrimidine-nucleotide salvage pathway. Unlike ordinary ones, UCK from *Thermus thermophilus* HB8 (ttCK) loses catalytic activity on Urd due to lack of a substrate binding ability and possesses an unusual amino acid, i.e. tyrosine 93 (Tyr93) at the binding site, whereas histidine (His) is located in the other UCKs. Mutagenesis experiments revealed that a replacement of Tyr93 by His or glutamine (Gln) recovered catalytic activity on Urd. However, the detailed molecular mechanism of the substrate specificity has remained unclear. In the present study, we performed molecular dynamics simulations on the wild-type ttCK, two mutant ttCKs, and a human UCK bound to Cyd and three protonation forms of Urd to elucidate their substrate specificity. We found three residues, Tyr88, Tyr/His/Gln93 and Arg152 in ttCKs, are important for recognizing the substrates. Arg152 contributes to induce a closed form of the binding site to retain the substrate, and the N3 atom of Urd needed to be deprotonated. Although Tyr88 tightly bound Cyd, it did not sufficiently bind Urd because of lack of the hydrogen bonding. His/Gln93 complemented the interaction of Tyr88 and raised the affinity of ttCK to Urd. The crucial distinction between Tyr and His or Gln was a role in the hydrogen-bonding network. Therefore, the ability to form both hydrogen-bonding donor and accepter is required to bind both Urd and Cyd.

Key words: molecular dynamics, binding free energy, deprotonated, keto-enol-enolate, hydrogen bond

Introduction

Nucleoside triphosphates (NTPs) are essential for organisms as energy sources and biosynthetic materials for nucleotides such as RNA and DNA. Since their complete biosyntheses from small molecules require a relatively high energy, the organisms recycle bases and nucleosides through a salvage pathway after consuming the NTPs. Uridine-cytidine kinase (UCK) is one of rate-limiting enzymes in the salvage pathway [1] and catalyzes the phosphorylation of two substrates, i.e., uridine (Urd) and cytidine (Cyd). UCK transfers the γ-phosphate groups in the adenosine triphosphate (ATP) to Urd or Cyd, and produces uridine monophosphate (UMP) or cytidine monophosphate (CMP), respectively. Subsequently, UMP and CMP are further phosphorylated by other

Corresponding author: Mitsuo Shoji, Center for Computational Sciences, University of Tsukuba, Tennodai 1-1-1, Tsukuba, Ibaraki 305-8577, Japan.
e-mail: mshoji@ccs.tsukuba.ac.jp

enzymes into uridine triphosphate (UTP) and cytidine triphosphate (CTP).

UCK has also attracted attention in a cancer treatment, because analogues of Urd and Cyd can act as its antimetabolite and suppress the growth of cancer cells by inhibiting the RNA synthesis. It was shown that the analogues must be triphosphorylated for the antimetabolic effect, and UCK catalyzes the initial phosphorylation of this process [2]. In this sense, UCK is recognized as a target protein for anti-cancer agents. Therefore, elucidating the substrate-binding mechanism of UCK is critically relevant not only for molecular biology, but also for cancer treatment.

Substrate-free and substrate analogue-bound structures of a human UCK were determined by X-ray experiments in 2004 [3]. In the latter structure, the substrate analogue is buried in a groove between the lid and β hairpin domains and forms a complex with UCK. In order to form the substrate-bound structure (closed form), two domains come close to each other to capture the substrate, and the substrate is then placed in a suitable position for the phosphorylation.

Unlike other UCKs, UCK taken from *Thermus thermophilus* HB8 (*Thermus thermophilus* UCK: ttCK) cannot act on Urd, but only on Cyd [4]. In the substrate-binding site of ttCK, tyrosine 93 (Tyr93), is located (see Fig. 1) in place of a histidine (His) commonly found in other UCKs. When the Tyr93 residue was replaced by His (Y93H) or glutamine (Y93Q), the catalytic activities of these mutants on both Urd and Cyd were recovered [4]. However, the molecular mechanism, i.e., why the 93rd amino acid residue highly influences the substrate specificity, is not clear at all.

For the bound Urd states, three different forms; the keto (k), enol (e) and deprotonated/enolate (d) states, were examined in the present study. Hereafter we abbreviated them as k-Urd, e-Urd, and d-Urd, respectively, for simplicity. Interactions between side chains of amino acids located in the binding site of WT ttCK and Cyd, k-Urd, e-Urd or d-Urd are schematically illustrated in Figure 2. When hydrogen atoms are attached to heavy elements in the crystal structure of the UTP-bound human UCK (PDBID: 1UEI) [3], a hydrogen atom on the N3 atom of k-Urd sterically conflicts with the side chain of Arg176. The same conflict was observed in k-Urd-bound ttCK (Fig. 2B). Therefore, Urd bound to UCK may be in other forms, i.e., e-Urd (Fig. 2C) or d-Urd (Fig. 2D), which have no hydrogen atoms on the N3 atom. The tautomerization energy of k-Urd into e-Urd in an aqueous solution is estimated to be 11.76 kcal mol^{-1} [5], and the deprotonation energy of k-Urd is approximated as 3.02 kcal mol^{-1} judging from the pK_a=9.2 of uridine. Thus, compared to the highly unstable e-Urd, d-Urd is slightly unstable compared to k-Urd in aqueous solutions.

In order to investigate the detailed molecular mechanism of the substrate specificity of the UCKs, we performed molecular dynamics (MD) simulations on the wild-type (WT) ttCK, two different ttCK mutants, and the human UCK with Urd and Cyd. For determining the binding free energy, the MM-PBSA approach was employed [6]. Based on these structural and energetic analyses, the substrate specificity of UCK and the roles of several amino acid residues including Tyr93 were elucidated. In the following section, the computational details are first given. The numerical results and discussion are then summarized in Sec. 2. Finally, the conclusions are listed in Sec. 3.

1. Materials and Methods

The starting structure of the WT ttCK with Cyd was taken

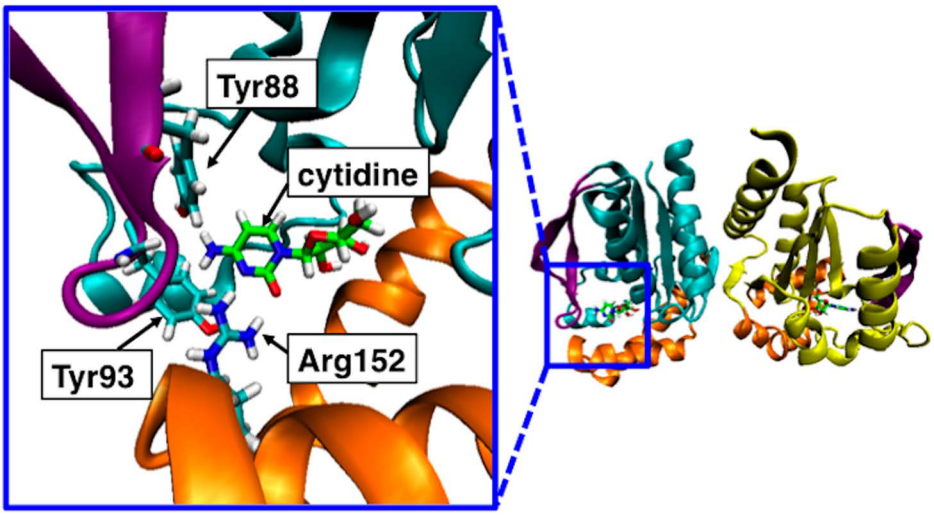

Figure 1 A structure of the binding site (left) and overall structure (right) of the WT ttCK binding cytidine (Cyd). The proteins are shown as ribbon models and Cyd, Tyr88, Tyr93, and Arg152 are shown as stick models. Each subunit of the dimer of ttCK is colored cyan and yellow. Cyd is colored green on its carbon atoms. The lid and β hairpin domains are colored orange and purple, respectively. All the structural images in this article are produced by VMD [15].

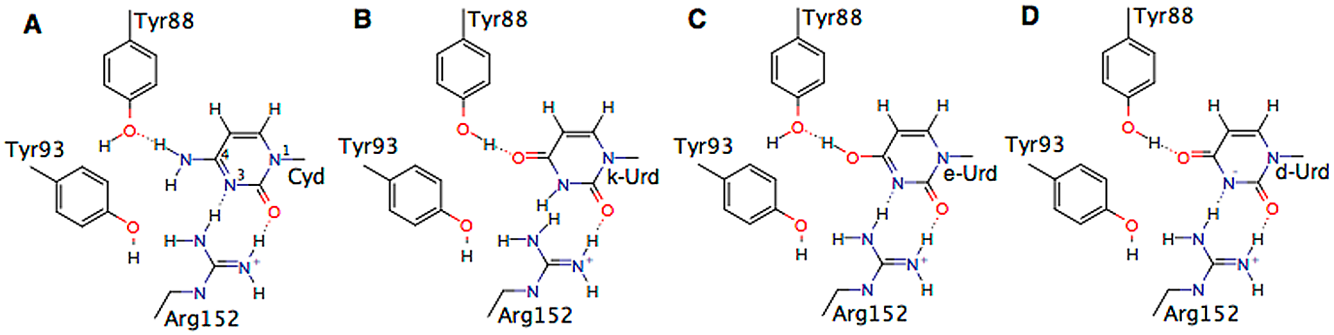

Figure 2 Interactions between the side chains of Tyr88, Tyr93, and Arg152 in WT ttCK and the base moiety of Cyd (A), k-Urd (B), e-Urd (C) or d-Urd (D). Hydrogen bonds are indicated by dotted lines.

from the crystal structure of the CMP-bound WT ttCK (PDBID: 3ASZ) [4] by deleting the phosphate group from CMP. The structures of the Y93H and Y93Q mutant ttCKs were manually constructed from the WT-ttCK model. The starting structure of the human UCK was obtained from the crystal structure of a human Cyd-bound UCK 2 (PDBID: 1UEJ) [3], and the six undetermined residues were provided using FREAD [7]. Side chains of His were set to be unprotonated in accordance with the pH=8.0 environment of the enzyme assay experiments [4]. The substrates examined in this study were Cyd and the three protonation states (k-, e-, and d-) of Urd. For these substrates, the General Amber Force Field (GAFF) parameters were adopted [8], in which the atomic charges of the substrates were determined by performing the B3LYP/6-31G(d) level calculation using the Gaussian09 program package [9] and by converting their charge density distributions to the RESP atomic charges using the Antechamber program in Amber 14 [10–12]. On the other hand, for the proteins, a general-purpose AMBER force field (ff14SB) was adopted. All the MD calculations were performed using the GROMACS 4.6 package [13]. We utilized the ACPYPE program [14] to convert the Amber input files to the GROMACS format. All the molecular images in this article were created by VMD [15].

The protein was initially placed in a periodic box of 95 Å×91 Å×93 Å size for the WT and mutant ttCKs or 82 Å×109 Å×94 Å size for the human UCK solvated with ~20000 TIP3P water molecules. Six or eight Cl^- ions were added to neutralize the net charge for the systems with d-Urd or other substrates, respectively. The particle-mesh Ewald (PME) method [16] with a 10 Å short range cut-off was employed. First, only the hydrogen atoms were optimized with constraints on the heavy atoms. The constant pressure ensemble (*NPT*) simulations at P=1 (bar), T=300 (K), and Δt=2 fs were then performed for 50 ns. Since the MD simulations were initiated on the substrate-binding crystal structures of UCKs, the systems reached steady structure based on RMSD values within 50 ns (see Supplementary Figure S1). The substrates came off the UCKs by 30 ns at latest when the complex structures were unstable. Thus, we regarded the 50-ns long MD simulations as enough to sample the complex structures. From the 10–50 ns MD trajectory data, the binding free energies (ΔG_B) were calculated by the MM-PBSA method using the MMPBSA.py program [6] in the AmberTools of Amber14. In the actual calculations, one subunit in the dimer of the UCK-substrate complex was used, and a continuous Poisson-Boltzmann model was adopted to take into account the solvation effects [17]. The entropy term was calculated by normal mode analysis and the contributions to the ΔG_B were evaluated by $T\Delta S$. In order to investigate fluctuations of the substrate in the binding site, ΔG_B was calculated from each 0.5 ns trajectory. For the detailed interaction analysis of ΔG_B between UCK and the substrates, a short-time trajectory (length of 4.8 ns from an arbitrary time point) was used. We checked that in the short-time trajectories, the substrates stayed in the binding site of UCK, so that the root mean square deviations (RMSDs) measured from the initial structures were not significantly changed. The averaged ΔG_B of the short-time trajectory was calculated every 20 ps. For the ΔG_B calculation of Urd, the tautomerization (ΔE_T=11.76 kcal mol^{-1}) and the deprotonation energy corrections (ΔE_P=3.02 kcal mol^{-1}) were added to ΔG_B for e-Urd and d-Urd, respectively.

2. Results and Discussion

2.1 Binding free energy and contribution of each residue

Depending on the substrates and UCKs, some substrates highly migrated from the initial binding site and the calculated ΔG_B fluctuated during the MD simulations. In order to show the intrinsic substrate binding feature and the distributions, scatter plots of ΔG_B vs. the substrate RMSD are shown in Figure 3, where ΔG_B was calculated using the MM-PBSA approach every 0.5 ns. Cyd was bound to all four types of UCKs with a low ΔG_B (–16 to 20 kcal mol^{-1}), and the substrate distributions were localized nearby its original binding position found in the crystal structure (RMSD=0.5–1.5 Å) (Fig. 3A). On the other hand, k-Urd had a relatively high ΔG_B for all the types of UCKs. Urd sometimes left the binding site of UCK and moved at most RMSD=9 Å from its

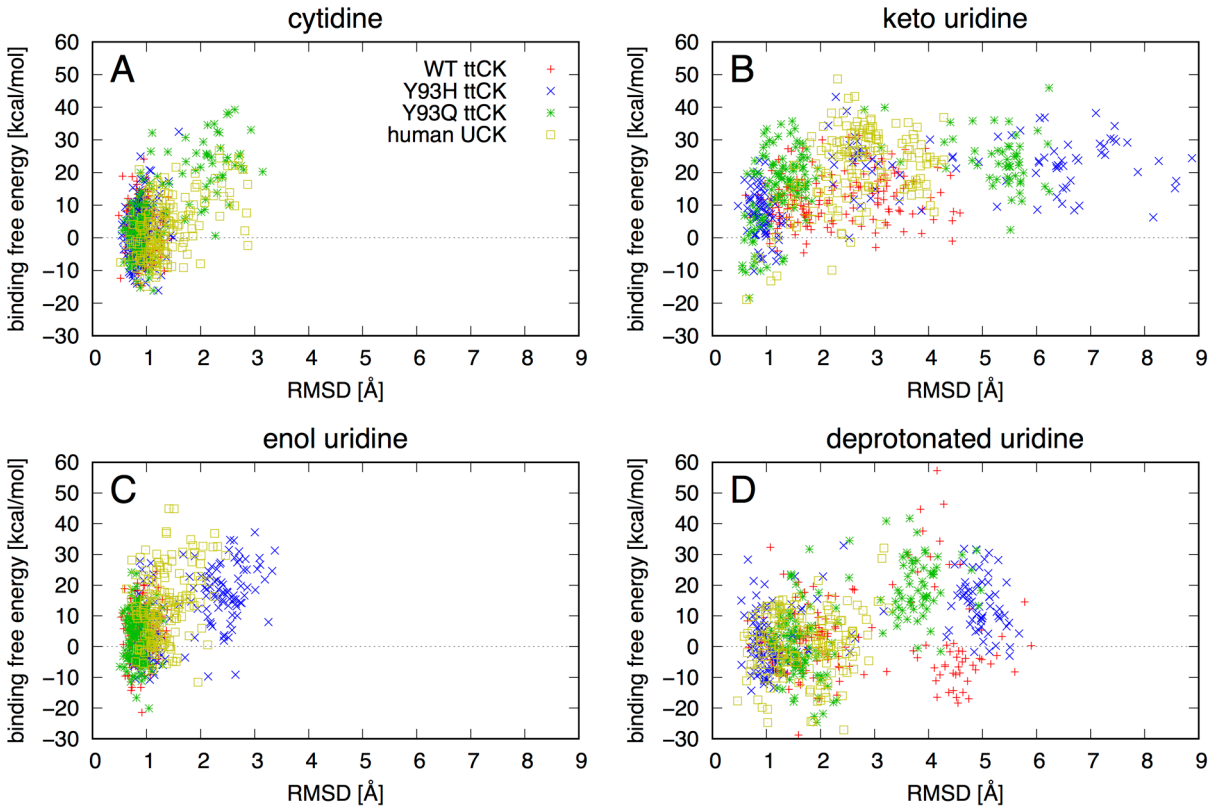

Figure 3 The binding free energy distributions of four types of UCK binding Cyd (A), k-Urd (B), e-Urd (C) and d-Urd (D) vs. RMSD of the substrates from its crystal structure. Both the energy and the RMSD were calculated at each 0.5 ns in the MD simulation and on each subunit of the dimer.

original position (Fig. 3B). The RMSD values nearly reached 5 Å, showing that k-Urd was not stable in all the UCKs. ΔG_B of e-Urd were comparable to that of Cyd (Fig. 3C). The RMSD values of e-Urd were mostly less than 3 Å. Based on these analyses, it is possible that the WT ttCK forms a stable complex with e-Urd, though this result is not consistent with the experimental results that the WT ttCK does not exhibit a catalytic activity on Urd [4]. Therefore, once e-Urd is formed in aqueous phase or in the catalytic pocket, it might be stabilized by WT ttCK. However, these reactions may not occur due to high potential barriers. For d-Urd, large distributions over ΔG_B=–15 to 15 kcal mol^{-1} and RMSD=1–3 Å (Fig. 3D) was observed. For human UCK, the binding energy of d-Urd is lower than those of k- and e-Urd. This result indicates that Urd is bound to UCKs in the d-Urd form. Note here that for the WT ttCK, the distribution around RMSD=4–5 Å were frequently observed and their ΔG_B values were low enough (–20 to 0 kcal mol^{-1}), which suggested that d-Urd could form a stable complex with the WT ttCK, but their binding states were not proper in the catalytic process. On the other hand, both for Y93H and Y93Q the distribution around RMSD=1–3 Å with low ΔG_B (–20 to 0 kcal mol^{-1}) were often observed, though another remarkable distribution is found around RMSD=4–5 Å with higher binding energy. This result suggests that Y93H and Y93Q bind to d-Urd.

The binding free energies, ΔG_B, between the UCKs and these substrates are summarized in Table 1, where the ΔG_B is defined as $\Delta G_B = G$ (complex)$-(G$ (substrate)$+G$ (protein)). These ΔG_B values were calculated using the short-time trajectories over 4.8 ns simulations when the substrates remained in the binding sites of UCK, even if the substrates were not tightly bound to UCKs. Judging from ΔG_B ranging from –4.82 to –0.52 kcal mol^{-1}, Cyd can bind to the four types of UCKs. Among ttCKs, the Y93H and Y93Q mutant ttCKs have higher binding affinities to Cyd than the WT does by 1.14 and 0.85 kcal mol^{-1}, respectively. In contrast, k-Urd

Table 1 Calculated binding free energy (ΔG_B in kcal mol^{-1}) for the substrates in the binding sites of UCKs. For the calculation, the time regions with a relatively small fluctuation and distortion of the substrates were selected

UCK		Cytidine (Cyd)	Uridine (Urd)		
			keto (k)	enol (e)[a]	deprotonated (d)[b]
ttCK	WT	–0.52	1.53	13.57	8.57
	Y93H	–1.66	2.87	11.46	0.15
	Y93Q	–1.37	7.67	10.80	–5.92
human UCK		–4.82	3.07	14.60	–2.75

[a] Correction for the tautomerization energy = 11.76 kcal mol^{-1} is included.
[b] Correction for the deprotonation energy = 3.02 kcal mol^{-1} is included.

showed low binding affinities with the four types of UCKs (ΔG_B=1.53 to 7.67 kcal mol^{-1}). Furthermore, k-Urd was not stably bound to the human UCK (ΔG_B=3.07 kcal mol^{-1}), which has a natural activity toward Urd. The positive ΔG_B of e-Urd for all cases indicates that the Urd does not take e-Urd form. We found that d-Urd substantially increased its affinities with the Y93H, Y93Q mutant ttCK and the human UCK compared to the WT ttCK (by 8.42, 14.49 and 11.32 kcal mol^{-1}, respectively). These results are consistent with the experiments that human UCK and mutant ttCKs can bind Urd. Because d-Urd is negatively charged and UCKs possesses some positively charged amino acid residues (Lys19, Arg142, Arg145, Arg150, and Arg152 in ttCK) near the active site, ΔG_B of d-Urd tended to be low due to the attractive electrostatic interaction between the negatively charged substrate and the positively charged amino acid residues. On the other hand, ΔG_B of d-Urd with the WT ttCK is still high (ΔG_B=8.57 kcal mol^{-1}) compared to ΔG_B of that with the mutant ttCKs and the human UCK. Thus, it can be considered that the mutations from Tyr93 to His or Gln play an important role in the substrate binding affinity. Thus we should further analyze the mutational effects on the structure and energetics in more detail.

In order to quantitatively evaluate the contribution of each amino acid residue to ΔG_B, we performed energy decomposition analyses on the results obtained by the MM-PBSA calculations [18]. It was found that eight amino acid residues mainly contributed to stabilizing the substrates (Figs. 4 and 5). In the Y93H mutant ttCK, Tyr59 and Phe90 interact with the substrate to form π-π stackings, and Ile113 interacts with the substrate via a hydrophobic interaction. Asp60 and Arg142 formed direct hydrogen bonds to the ribose moiety of the substrate, and Tyr88, His93, and Arg152 formed hydrogen bonds to the base moiety of the substrate. It is noteworthy that Arg152 (Arg176 in the human UCK) showed a positive ΔG_B to the k-Urd (Fig. 5B). Tyr88 (Tyr112 in the human UCK) also showed a negative ΔG_B to Cyd in the four types of UCKs. However, Tyr88 (Tyr112) reduced the contribution to the three types of Urds in some UCKs, i.e., k-Urd in the human UCK, e-Urd in the Y93H and Y93Q mutant ttCKs, and d-Urd in the Y93Q mutant ttCK (Fig. 5B, C, D). Therefore, we regarded Arg152 and Tyr88 (Arg176 and Tyr112 in human UCK) as key amino acid residues in the substrate specificity of UCK. The roles of these residues and Tyr/His/Gln93 (His117 in human UCK) are discussed below.

2.2 Roles of Arg152 in ttCK

The k-Urd showed a low affinity with the four types of UCKs (Table 1), and the repulsive interactions with Arg152 (or Arg176 in the human UCK) were significantly observed (Fig. 5B). Thus, Arg152 is the major reason for the low affinity of k-Urd, which has the H atom bound to the N3 atom in its base moiety. This H atom repels the side chain of Arg152. In the MD simulations, when the repulsive interaction exists, UCK could not keep the closed-form structure capturing

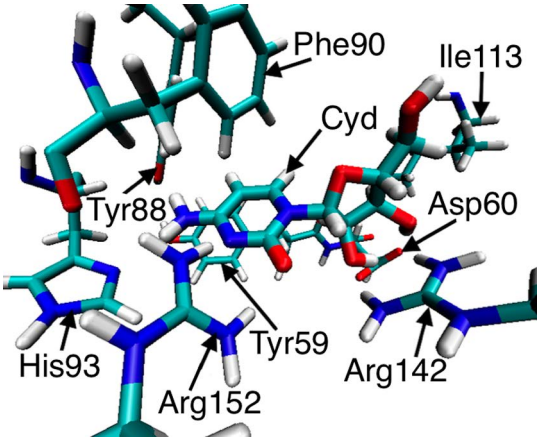

Figure 4 The amino acid orientations at the binding site of the Cyd-binding Y93H ttCK obtained from the MD simulation. Tyr59 and Phe90 form π-π stackings and CH-π interaction with Cyd, and Ile113 interacts with Cyd via a hydrophobic interaction. Tyr88, His93, and Arg152 form hydrogen bonds with the Cyd base moiety, and Asp60 and Arg142 anchor the ribose moiety.

Urd (Fig. 6). The distance between the lid and the β hairpin domains increased roughly from 5 to 10–15 Å during the simulation, and Urd left the binding site of UCK. Therefore, an attractive interaction between Arg152 (or Arg176) and a substrate is crucial for the substrate binding of UCK. In the crystal structure of the human UCK binding UTP (PDBID: 1UEI) [3], the position of the H atom bound to N3 is too close to the side chain of Arg176. Because the pK_a values of Arg and Urd are 12.1 and 9.2, respectively, Urd was considered to be in the deprotonated form.

2.3 The role of His/Gln93 complementing the interaction between Tyr88 and the substrate

Tyr88 can form a hydrogen bond with the amino group on the C4 atom of Cyd (see Fig. 2) or the carbonyl group of Urd as an acceptor or a donor, respectively. During the simulations, Tyr88 sufficiently stabilized the Cyd, but could not sufficiently bind k- and e-Urds to keep it in the active site. In the case of d-Urd, the direction of the hydroxyl group in Tyr88 frequently changed (Fig. 7). This means that the hydrogen bond was not continuously formed with the substrates. There was another carbonyl group of the Lys44 backbone in the opposite direction from the substrate (Fig. 8). When Tyr88 made a hydrogen bond with Lys44, Tyr88 could not make a hydrogen bond with d-Urd (Fig. 8C), but could with Cyd (Fig. 8A), because both the carbonyl group of the Lys44 backbone and d-Urd were hydrogen-bond acceptors (Fig. 8B and C). Consequently, d-Urd lost its attractive interactions with the binding site and moved away from the binding site in the case of WT ttCK.

To keep Urd at the binding site, it is necessary for another interaction to hold Urd. Although Tyr93 was located at the proper position in the WT ttCK, its side chain was too large and could bind neither Cyd nor Urd (Fig. 9A and B). On the

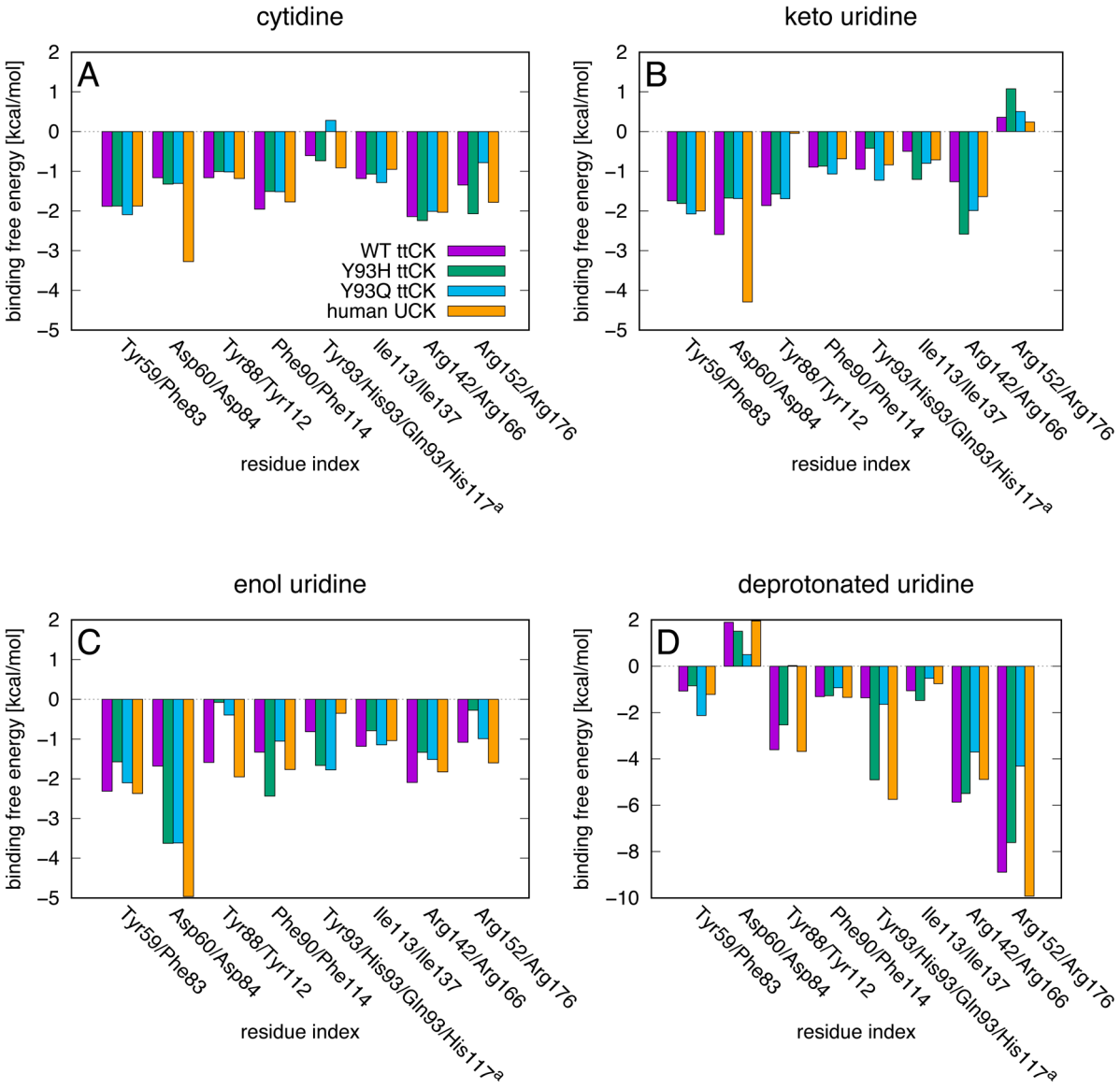

Figure 5 The binding free energy contributions from the dominant eight amino acids in the UCKs. Note that residue indexes are given for WT and mutant ttCKs/human UCK. The residue indexes with a superscript (a) indicate for WT ttCK/Y93H ttCK/Y93Q ttCK/human UCK.

other hand, His93 was also located at the proper position in the Y93H ttCK mutant (Fig. 4) and had a side chain with a suitable size. This could be used as both a hydrogen-bond acceptor and donor by transferring its H atom between the ε- and δ-positions (Fig. 9C and D) or rotating its side chain. The same mechanism was true for His117 in the human UCK [3]. Gln93 in the Y93Q ttCK mutant also played a key role in serving as a hydrogen-bond acceptor or donor, because it contained both a carbonyl group and an amino group (Fig. 9E and F). Due to the positions of its carbonyl and amino groups, Gln93 also could form hydrogen bonds with Tyr88 and d-Urd at the same time (Fig. 9F). Since His/Gln93 could simultaneously bind Cyd with Tyr88, the Y93H and Y93Q ttCK mutants further gain a higher affinity to Cyd than the WT even if the WT already had a certain affinity to Cyd. Therefore, to bind both substrates, i.e., Cyd and Urd, UCK needs a key amino acid residue having the following two characteristics: (1) the proper small size of its side chain, and (2) a geminal hydrogen-bonding ability to behave both as a hydrogen-bond acceptor and donor. Both His and Gln satisfy these requirements.

3. Conclusion

The detailed molecular mechanisms of the substrate specificity of UCK were investigated by MD simulations and binding free energy analyses. Based on these analyses, Urd was bound to ttCK in the deprotonated form in the present

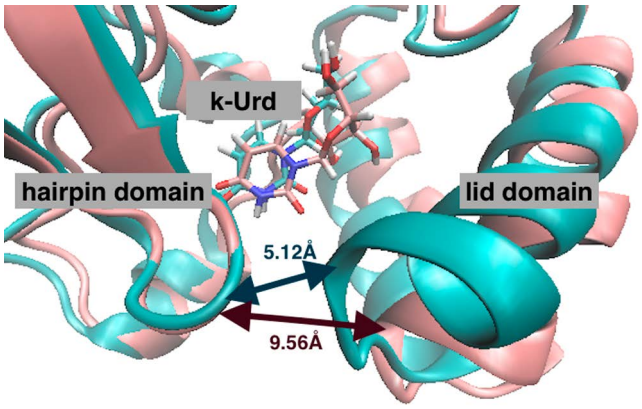

Figure 6 The distance between lid and β hairpin domains of ttCK increased when binding the k-Urd. The initial structure and the final structure of the 50 ns MD simulation are colored cyan and pink, respectively.

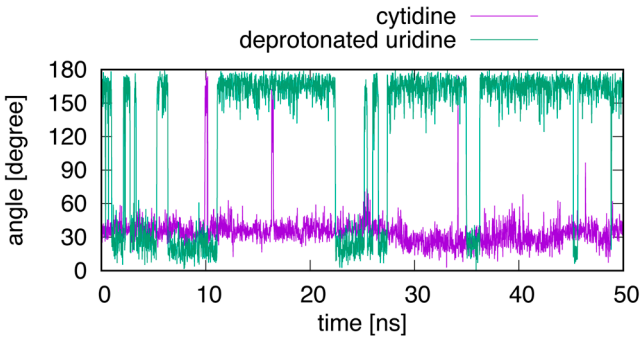

Figure 7 The angle of O (hydroxyl group of Tyr88)–H (hydroxyl group of Tyr88)–N (amino group of cytidine) or O (carbonyl group of uridine). An angle of around 30 or 180 degrees indicates that Tyr88 serves as a hydrogen-bond acceptor or donor, respectively. While Tyr88 kept the hydrogen bond with Cyd mostly over the simulation (purple), it frequently lost the bond with Urd (green).

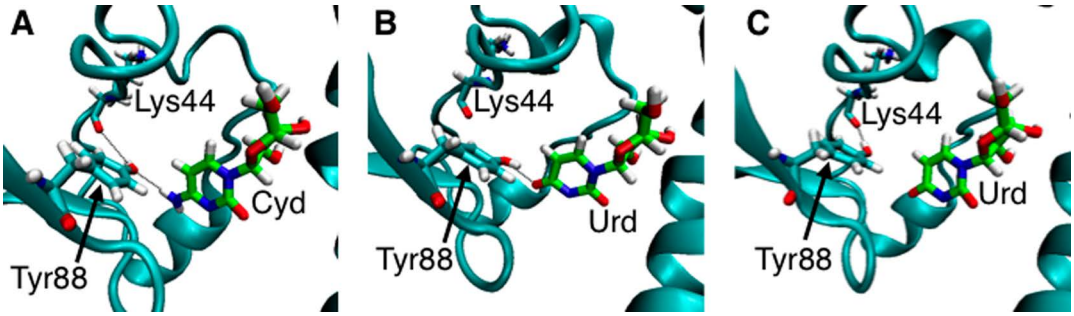

Figure 8 A backbone carbonyl group of Lys44 located near Tyr88 which binds both the carbonyl group and Cyd (A). In the case with Urd, Tyr88 binds either Urd (B) or the carbonyl group of Lys44 (C).

study, though the natural form of Urd in the aqueous phase is the keto form. Three amino acid residues in ttCK, Tyr88, Tyr/His/Gln93 and Arg152, were found to be crucial for recognition of the substrates. Arg152 bound and enveloped the substrate by keeping the lid and β domains closed to form a stable complex. Tyr88 could stably bind the amino group on the C4 atom of Cyd as a hydrogen-bond acceptor. However, it could not bind the carbonyl group of d-Urd as a donor, because another carbonyl group of Lys44 exists near the hydroxyl group of Tyr88 to form the hydrogen bond. Since the carbonyl group of d-Urd was held only by Tyr88 in the WT ttCK, d-Urd easily lost its hydrogen-bonding interaction with the WT ttCK. Indeed, d-Urd was released in the MD simulation. By replacing Tyr93 with His or Gln, the residue can interact with d-Urd and recover the binding ability due to forming hydrogen bonds. Since His93 and Gln93 exhibited the abilities to behave both as an acceptor and a donor, they could bind both Cyd and Urd.

Acknowledgements

Numerical calculations have been carried out under the support of (1) "Interdisciplinary Computational Science Program" at the Center for Computational Sciences, University of Tsukuba; (2) the HA-PACS Project for advanced interdisciplinary computational sciences by exa-scale computing technology. This research was supported by MEXT/JSPS KAKENHI (Grant-in-Aid for Scientific Research (C) No. 26410002 and Grant-in-Aid for Scientific Research on Innovative Areas; Nos. 26102525 and 26107004).

Conflicts of Interests

W.T., M.S., F.T., Y.U., K.H., R.H., M.K., K.K., T.I., R.M., S.K. and Y.S. declare that they have no conflict of interest.

Author Contributions

W.T. performed theoretical calculations. M.S., F.T., Y.U., K.H., R.H., M.K., K.K. T.I., R.M., S.K. and Y.S. assisted his calculations and advised for his theoretical analyses. W.T, M.S., Y.S. wrote the paper. M.S., S.K. and Y.S. directed the project.

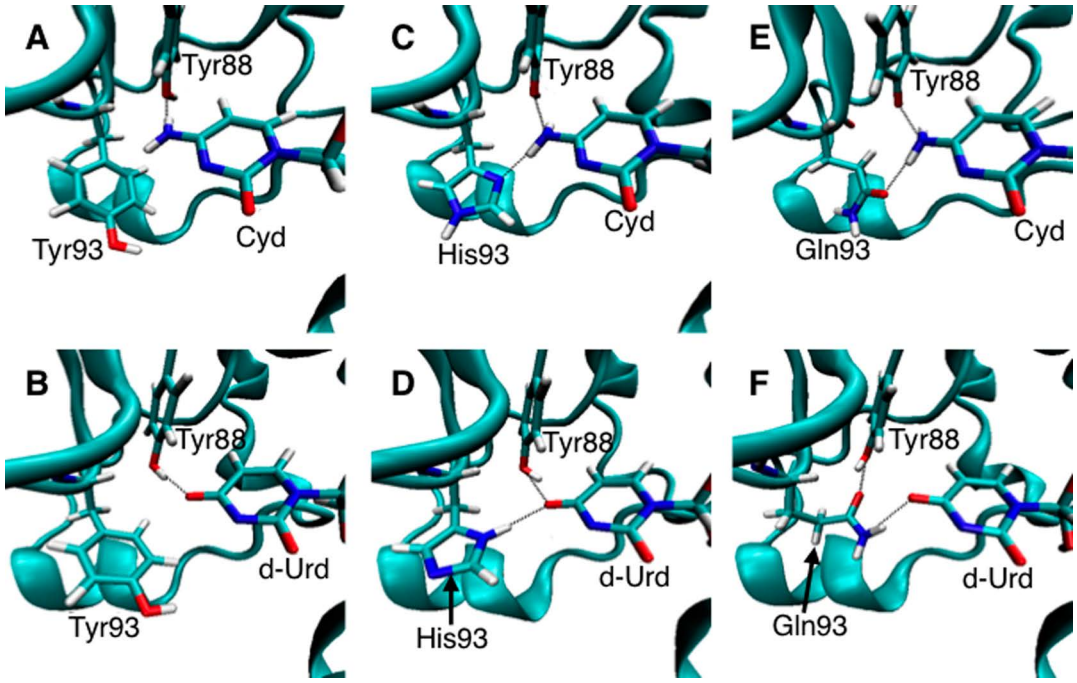

Figure 9 The interactions of Tyr88 and Tyr93 with Cyd (A) or Urd (B); His93 with Cyd (C) or Urd (D); Gln93 with Cyd (E) or Urd (F). Tyr93 completely lost the hydrogen-bonding interaction with the substrates. His/Gln93 simultaneously bound the substrates with Tyr88.

References

[1] Anderson, E. P. & Brockman, R. W. Feedback inhibition of uridine kinase by cytidine triphosphate and uridine triphosphate. *Biochim. Biophys. Acta* **91**, 380–386 (1964).

[2] Tabata, S., Tanaka, M., Endo, Y., Obata, T., Matsuda, A. & Sasaki, T. Anti-tumor mechanisms of 3′-ethynyluridine and 3′-ethynylcytidine as RNA synthesis inhibitors: development and characterization of 3′-ethynyluridine-resistant cells. *Cancer Lett.* **116**, 225–231 (1997).

[3] Suzuki, N. N., Koizumi, K., Fukushima, M., Matsuda, A. & Inagaki, F. Structural basis for the specificity, catalysis, and regulation of human uridine-cytidine kinase. *Structure* **12**, 751–764 (2004).

[4] Tomoike, F., Nakagawa, N., Kuramitsu, S. & Masui, R. A single amino acid limits the substrate specificity of *Thermus thermophilus* uridine-cytidine kinase to cytidine. *Biochemistry* **50**, 4597–4607 (2011).

[5] Kryachko, E. S., Nguyen, M. T. & Zeegers-Huyskens, T. Theoretical study of tautomeric forms of uracil. 1. relative order of stabilities and their relation to proton affinities and deprotonation enthalpies. *J. Phys. Chem. A* **105**, 1288–1295 (2001).

[6] Miller, B. R., McGee, T. D., Jr., Swails, J. M., Homeyer, N., Gohlke, H. & Roitberg, A. E. MMPBSA.py: An efficient program for end-state free energy calculations. *J. Chem. Theory Comput.* **8**, 3314–3321 (2012).

[7] Choi, Y. & Deane, C. M. FREAD revisited: Accurate loop structure prediction using a database search algorithm. *Proteins* **78**, 1431–1440 (2010).

[8] Wang, J., Wolf, R. M., Caldwell, J. W., Kollman, P. A. & Case, D. A. Development and testing of a general amber force field. *J. Comput. Chem.* **25**, 1157–1174 (2004).

[9] Frisch, M. J., Trucks, G. W., Schlegel, H. B., Scuseria, G. E., Robb, M. A., Cheeseman, J. R. *et al.* Gaussian 09, Revision A.02 (2009).

[10] Bayly, C. I., Cieplak, P., Cornell, W. D. & Kollman, P. A. A well-behaved electrostatic potential based method using charge restraints for deriving atomic charges: The RESP model. *J. Phys. Chem.* **97**, 10269–10280 (1993).

[11] Wang, J., Wang, W., Kollman, P. A. & Case, D. A. Automatic atom type and bond type perception in molecular mechanical calculations. *J. Mol. Graph. Model.* **25**, 247–260 (2006).

[12] Case, D. A., Babin, V., Berryman, J. T., Betz, R. M., Cai, Q., Cerutti, D. S. *et al.* AMBER 14. University of California, San Francisco (2014).

[13] Van der Spoel, D., Lindahl, E. & Hess, B. The GROMACS development team GROMACS User Manual version 4.6.5. www.gromacs.org (2013).

[14] Sousa da Silva, A. W. & Vranken, W. F. ACPYPE—AnteChamber PYthon Parser interfacE. *BMC Res. Notes* **5**, 367–374 (2012).

[15] Humphrey, W., Dalke, A. & Schulten, K. VMD—Visual Molecular Dynamics. *J. Mol. Graph.* **14**, 33–38 (1996).

[16] Darden, T., York, D. & Pedersen, L. Particle mesh Ewald: An $N\cdot\log(N)$ method for Ewald sums in large systems. *J. Chem. Phys.* **98**, 10089–10092 (1993).

[17] Homeyer, N. & Gohlke, H. Free energy calculations by the molecular mechanics Poisson-Boltzmann surface area method. *Mol. Inform.* **31**, 114–122 (2012).

[18] Gohlke, H., Kiel, C. & Case, D. A. Insights into protein-protein binding by binding free energy calculation and free energy decomposition for the Ras-Raf and Ras-RalGDS complexes. *J. Mol. Biol.* **330**, 891–913 (2003).